Cancer Immunology, Immunotherapy

Göthert et al.

Supplementary tables

Table S1. Patient characteristics.

Parameters	***No. of patients (%)***
Total number of patients	*105 (100)*
Male/ female	*69/36 (66/34)*
Binet stage (n=104)	
A	*61 (59)*
B	*27 (26)*
C	*16 (15)*
CD38 expression (n=103)	
positive	*38 (37)*
negative	*65 (63)*
Genomic aberrations by FISH (n=94)	
No	*21 (22)*
Deletion 13	*51 (54)*
Deletion 11q	*8 (9)*
Trisomy12	*11 (12)*
Deletion 17p	*3 (3)*
Treatment history	
treated	*10 (9)*
untreated	95 (91)

Table S2. Correlations between peripheral blood cellular subset dynamics.

		lymphocytes	*CD3*	*CD4*	*CD8*	*NK*
lymphocytes	r_s	***1.00***	*0.59*	*0.51*	*0.59*	*0.36*
	P value		*<0.0001*	*<0.0001*	*<0.0001*	*0.048*
CD3	r_s	*0,59*	***1.00***	*0.87*	*0.94*	*0.25*
	P value	*<0.0001*		*<0.0001*	*<0.0001*	*0.19*
CD4	r_s	*0.51*	*0.87*	***1,00***	*0,80*	*0.25*
	P value	*<0.0001*	*<0.0001*		*<0.0001*	*0.18*
CD8	r_s	*0.59*	*0.94*	*0.80*	***1,00***	*0.29*
	P value	*<0.0001*	*<0.0001*	*<0.0001*		*0.12*
NK	r_s	*0.36*	*0.25*	*0,25*	*0.29*	***1,00***
	P value	*0.048*	*0.19*	*0.18*	*0.12*	

Individual patient cellular subset dynamics were determined as cellular increments/ µl per month as outlined in Figure 1A. The calculations of Spearman correlation coefficients (r_s) included n=46 CLL patients.

Table S3. Differentially expressed probes of CLL vs. Normal donor derived CD3-purified T-cell samples.

Gene ID	Affymetrix ID	Fold Change
TCF4	213891_s_at	7,42
IGHM	212827_at	4,29
IGHM	209374_s_at	4,93
C13orf18	219471_at	6,87
TCF4	212386_at	6,93
FCGR2B	210889_s_at	3,45
TCF4	203753_at	4,99
HLA-DQA1	203290_at	7,67
HLA-DRB1	215193_x_at	2,39
HLA-DRA	208894_at	2,41
VCAM1	203868_s_at	3,05
SCD	200832_s_at	2,6
TRGV9	209813_x_at	2,82
TNFRSF9	207536_s_at	2,29
RAB7L1	218699_at	2,03
SH2D1A	211209_x_at	2,08
C13orf18	44790_s_at	5,08
C16orf5	218183_at	2,36
PAX5	221969_at	2,49
KIF11	204444_at	3,27
TARP	216920_s_at	2,86
TRGC2	215806_x_at	2,71
PRF1	214617_at	3,26
CST7	210140_at	2,48
RUVBL1	201614_s_at	2,11
CD58	216942_s_at	2,13
HLA-DPA1	211991_s_at	2,14
TARP	211144_x_at	2,7
POU2AF1	205267_at	2,11
PLCG2	204613_at	2,63
GTF2H5	213357_at	2,08
APOBEC3F	214995_s_at	2,41
MPV17	203466_at	2,15

Gene ID	Affymetrix ID	Fold Change
HLA-DRB1	209312_x_at	2,12
SMARCAL1	218452_at	2,58
ELP3	221094_s_at	2
C11orf49	203257_s_at	2,2
GZMK	206666_at	2,14
NINJ2	219594_at	2,4
CRTAM	206914_at	2,22
CLIC3	219529_at	3,48
HLA-DQA1	212671_s_at	3,55
MED12	211342_x_at	2,13
PTGDR	215894_at	2,35
RALBP1	202844_s_at	2,89
PVRIG	219812_at	2,14
CTSC	201487_at	2,19
RBM8A	217857_s_at	3,34
STIP1	212009_s_at	2,13
DNAJB6	209015_s_at	2,56
DYNLL1	200703_at	2,16
METTL7A	207761_s_at	2,2
LPCAT1	201818_at	2,56
PLEK	203470_s_at	2,54
MYCBP	203360_s_at	2,15
IDH1	201193_at	2,19
OAS2	206553_at	2,4
CD244	220307_at	2,43
HEMK1	218620_s_at	2,33
DMN	212730_at	2,05
DPYSL2	200762_at	2,04
CD160	207840_at	2,9
KLRF1	220646_s_at	2,51
CHST12	218927_s_at	2,19
ARPC4	217818_s_at	2,4
RAD51C	209849_s_at	2,7

Gene ID	Affymetrix ID	Fold Change
GZMA	205488_at	2,44
FLJ14213	219383_at	2,55
ARPC5	211963_s_at	2,03
M6PR	200900_s_at	2,15
CCL4	204103_at	2,68
ARFIP1	214483_s_at	2,24
ANXA4	201301_s_at	2,91
CCR5	206991_s_at	3,72
FGR	208438_s_at	2,32
MELK	204825_at	2,05
CRIPT	218643_s_at	2,99
KLRA1	207229_at	2,11
ATP6V1D	208898_at	2,15
RNF5	209111_at	2,07
C3orf60	209177_at	2,86
PTGDS	211748_x_at	3,45
PLEK	203471_s_at	2,14
HLA-DRA	210982_s_at	2,52
ARFIP1	218230_at	3,39
ST8SIA1	210073_at	2,45
PIGN	219048_at	2,65
STX7	212631_at	2,14
RRM2	201890_at	2,8
FADS2	202218_s_at	2,43
ADCY9	204497_at	2,18
ENSA	221487_s_at	2,04
RRBP1	201204_s_at	2,25
WIPI1	213836_s_at	2,31
APOBEC3G	204205_at	2,12
GOLPH3L	218361_at	3,42
SMC2	204240_s_at	2,31
CX3CR1	205898_at	4,06
KLRK1	205821_at	2,14
FASTKD1	219002_at	2,01
NKG7	213915_at	2,15
TKTL1	214183_s_at	2,45
COL4A3	222073_at	2,06
DENND2D	221081_s_at	2,27
PECAM1	208983_s_at	2,25
RPE	221770_at	2,23
RALBP1	202845_s_at	2,01
PCMT1	205202_at	2,03
TAF1B	214690_at	2,11
CD79B	205297_s_at	2,01
PTGER2	206631_at	2,08
BTN3A2	212613_at	2,45
SEC23B	201582_at	2,03
AOAH	205639_at	2,09
SNX1	214531_s_at	2,37
CD300A	209933_s_at	2,66

Gene ID	Affymetrix ID	Fold Change
JAKMIP2	205888_s_at	2,16
FARSA	216602_s_at	2,87
SELPLG	209880_s_at	2,07
ACADM	202502_at	2,08
KLRD1	210606_x_at	2,49
IGKC	221651_x_at	4,19
KLRC2	206785_s_at	3,3
ANXA4	201302_at	2,08
BID	204493_at	2,08
ZMYM6	219924_s_at	2,07
TTC38	218272_at	3,43
AQR	212583_at	2,14
TNFRSF1A	207643_s_at	2,08
SH3BP2	217257_at	2,19
SKAP2	204362_at	2,35
SLCO4C1	222071_s_at	2,36
CTNNA1	210844_x_at	2,25
GIMAP4	219243_at	2,75
C1orf103	220235_s_at	2,09
KLRD1	207795_s_at	2,28
FLJ11151	218610_s_at	2,21
SKAP2	204361_s_at	2,25
TSPAN31	203227_s_at	2,01
SEC23IP	216392_s_at	2,52
NA	220577_at	2
HSDL2	209512_at	2,15
HLA-DQB1	212998_x_at	2,28
PPP1R10	201702_s_at	2,41
LPCAT4	40472_at	2,07
PDE6D	216883_x_at	2,45
NDUFAF1	204125_at	2,02
DLGAP5	203764_at	2,32
IGL@	215121_x_at	2,29
ALDH5A1	203608_at	2,08
PPBP	214146_s_at	0,15
NA	215392_at	0,44
MEIS3P1	214077_x_at	0,5
IRS2	209185_s_at	0,34
IRS2	209184_s_at	0,41
PGAP1	220576_at	0,46
BACH1	204194_at	0,48
SCML1	218793_s_at	0,27
CSGALNACT1	219049_at	0,5
FBXL11	208989_s_at	0,47
SGK1	201739_at	0,26
NET1	201830_s_at	0,44
ZBTB10	219312_s_at	0,38

Table S4. The differentially expressed T-cell genes were further analyzed for associations with biological processes as defined in the Gene Ontology (GO) data base.

GOBPID	Pvalue	Count	Size	Term
GO:0006955	5,57E-08	22	289	immune response
GO:0002376	1,18E-06	24	401	immune system process
GO:0002504	2,28E-06	5	12	antigen processing and presentation of peptide or polysaccharide antigen via MHC class II
GO:0050896	4,48E-06	41	1018	response to stimulus
GO:0031347	4,46E-05	6	33	regulation of defense response
GO:0006968	8,76E-05	6	37	cellular defense response
GO:0048583	0,00013923	8	76	regulation of response to stimulus
GO:0019882	0,00015853	6	41	antigen processing and presentation
GO:0006952	0,00040894	13	216	defense response
GO:0002230	0,00041225	2	2	positive regulation of defense response to virus by host
GO:0006410	0,00041225	2	2	transcription, RNA-dependent
GO:0045869	0,00041225	2	2	negative regulation of retroviral genome replication

Supplementary figure

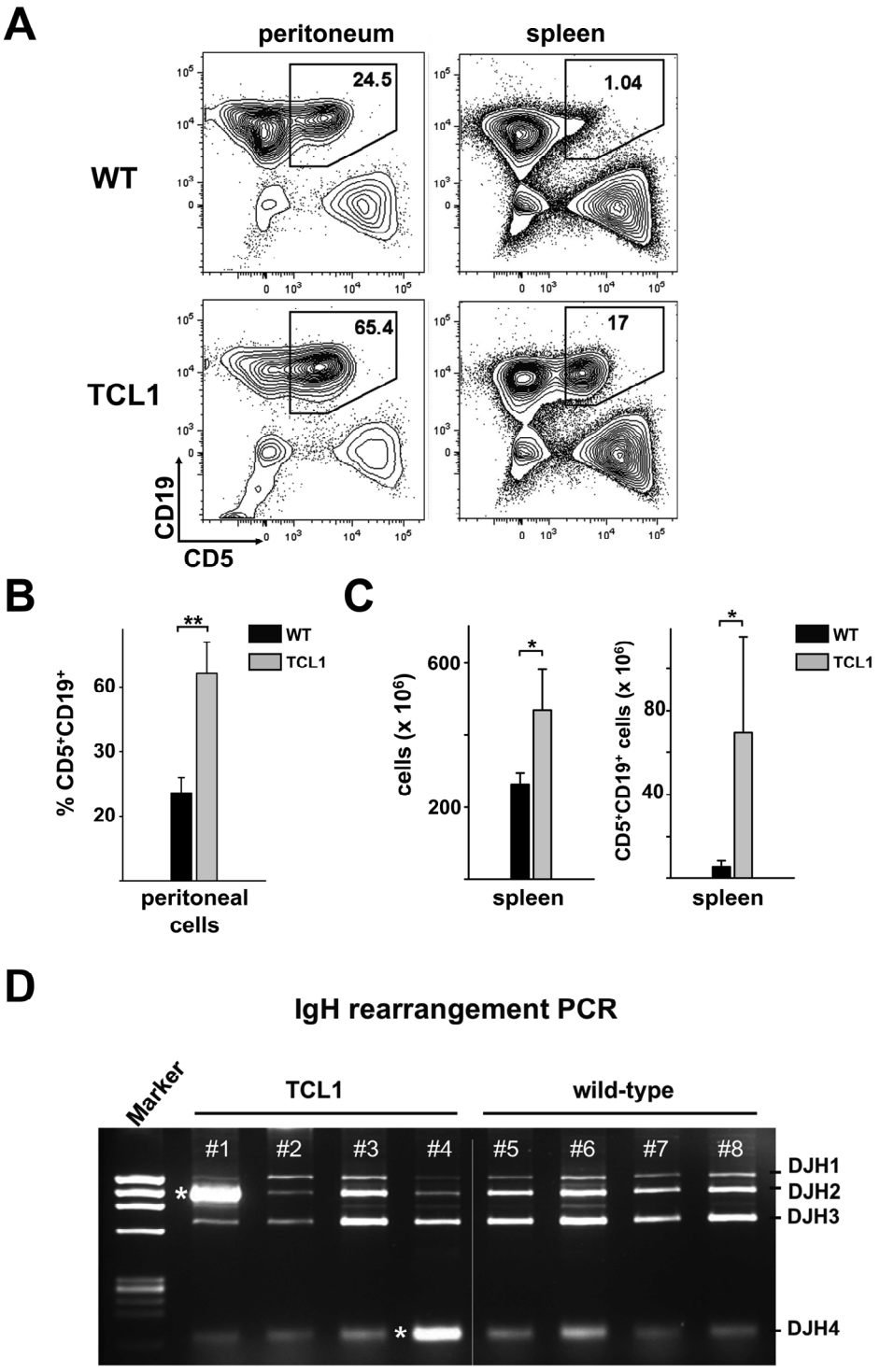

Figure S1. Emergence of CLL-like disease in 7-month-old TCL1 transgenic mice. (A) Expansion of the peritoneal and splenic $CD5^+CD19^+$ B-cell compartment in TCL1 transgenic mice compared to wild-type controls. Representative plots are displayed. (B) The percentage of peritoneal $CD5^+CD19^+$ cells (gated as shown in A) of TCL1 transgenic (n=4) compared to wild-type mice (n=6) is significantly increased. (C) Quantification of total splenic cells and $CD5^+CD19^+$ cells per spleen. TCL1

transgenic mice (n=4) were compared to wild-type control mice (n=6). (D) In parallel to the flow cytometric analysis we isolated DNA from splenocytes and carried out a previously published clonality PCR [1-3]. IgH locus rearrangement converges DSF and J_H4 primer annealing sites. DSF is a degenerate forward Primer specific for recombination signal sequences upstream of D_H Segments (DSF; sequence AGG GAT CCT TGT GAA GGG ATC TAC TAC TGT G). J_H4 is a reverse primer specific for the J_H4 segment (J_H4, AAA GAC CTG CAG AGG CCA TTC TTA CC). In normal polyclonal B-cell populations this PCR amplifies 4 different rearranged DJ_H segments. In oligoclonal or monoclonal populations preferential amplification or loss of segments can occur. Asterisks on the displayed gel image depict preferentially amplified DJ_H segments. The gel image demonstrates emerging clones in TCL1 spleens #1 and #4.

Supplementary references

1. Sollbach AE, Wu GE (1995) Inversions produced during V(D)J rearrangement at IgH, the immunoglobulin heavy-chain locus. Mol Cell Biol 15(2): 671-681

2. Kawamoto H, Ikawa T, Ohmura K, Fujimoto S, Katsura Y (2000) T cell progenitors emerge earlier than B cell progenitors in the murine fetal liver. Immunity 12(4): 441-450

3. Chang Y, Paige CJ, Wu GE (1992) Enumeration and characterization of DJH structures in mouse fetal liver. EMBO J 11(5): 1891-1899